

A NEW MULTI-HARMONIC LOAD-PULL METHOD
FOR NON LINEAR DEVICE CHARACTERIZATION AND MODELING

Robert Larose, Fadhel M. Ghannouchi, Renato G. Bosisio

Microwave Research Laboratory, Electrical Engineering Department
ÉCOLE POLYTECHNIQUE DE MONTREAL
P. O. Box 6079, Station A, Montreal, Que., H3C 3A7
Tel: (514) 340-4872 - FAX: (514) 340-4147

ABSTRACT

A new multi-harmonic load-pull system based on an active load tuning configuration is presented. The system allows independent load-tuning of an excitation signal and its harmonics. Load-pull measurements on MESFET (NEC 71083) have been performed at the fundamental (f_0), second ($2f_0$), and third ($3f_0$) harmonics. The results show the importance of such measurements in designing and modeling non linear devices and circuits.

INTRODUCTION

The trend towards better large-signal modeling of active devices triggers the need for simple and pertinent non-linear measurements. Methods like load-pull using automatic tuners [1], active load-pull [2], harmonic load-pull [3], and measurement of amplitude and phase of harmonics [4], provide a good insight on non linear elements in various models.

The present paper illustrates a new characterization system to investigate harmonic load-tuning using second and third harmonics of the excitation signal with a wide-band six-port network analyzer [5,6] in an active load-pull configuration [7]. Constant output power $P(f_0)$ contours were obtained in variable complex $\Gamma_L(f_0)$ plane for chosen values of $\Gamma_L(2f_0)$ and $\Gamma_L(3f_0)$. Similarly constant power contours for $P(2f_0)$ were obtained in a variable complex $\Gamma_L(f_0)$ plane with chosen and fixed values of $\Gamma_L(2f_0)$ and $\Gamma_L(3f_0)$. In addition two other test conditions of the total nine possible test conditions for the fundamental, second and third harmonics are presented. More harmonics could be used by this test method by upgrading the measurement system. Table I below indicates the four tests presented in this paper.

TABLE I

Harmonic Power Harmonic Contour Complex Plane	$P_L(f_0)$	$P_L(2f_0)$	$P_L(3f_0)$
$\Gamma_L(f_0)$	x	x	
$\Gamma_L(2f_0)$		x	
$\Gamma_L(3f_0)$			x

Fixed values of Γ_L in the non-test harmonic plane were chosen and kept constant during the measurements, such as to satisfy a given design criteria (e.g. minimum or maximum power level at a given harmonic). Experimental results were found to be directly applicable to frequency multipliers and high power amplifier design.

MEASUREMENT SYSTEM

The experimental set-up for active load-pull measurements is similar to the set-up used with a dual six-port network analyzer. Each six-port reflectometer SP1 and SP2 was calibrated independently for impedance and power flow measurements over a 2-12 GHz frequency band. The feasibility of a dual six-port network analyzer in a load-pull system with an active single frequency load-tuning configuration, has been proved in a previous paper [4]. It is important to notice that a six-port junction is a linear network, thereby multi-frequency signals can be handled by a six-port junction; impedance measurements at each frequency can be performed using appropriate dividing/filtering circuits before power detection. Input excitation frequency signal f_0 , second harmonic $2f_0$ and

third harmonic $3f_o$ are injected simultaneously at the input of the second six-port junction SP2 by means of a three-way power combiner as shown in Figure 1. A variable attenuator and variable phase shifter are inserted in the fundamental branch (between the three-way power combiner and the directional coupler DC1) to change the simulated load impedance seen by the transistor at f_o . The second (third) harmonic branch includes a frequency doubler (tripler) and amplitude and phase controllers as required to synthesize the desired second (third) harmonic impedance to be seen by the microwave transistor operating in a non linear mode. Three narrowband isolators (one in each branch) are used to facilitate independent harmonic impedance tuning. At each detection port of SP2, the multi-frequency signal is split in three parts using a wideband three-way unequal power divider, three bandpass filters centered respectively at f_o , $2f_o$ and $3f_o$ are used to recover selectively the signals at f_o , at $2f_o$ and at $3f_o$, from the multi-frequency signal. The output of these bandpass filters are connected to three four-channel power meters as shown in Figure 1. A high power amplifier is inserted at the output of the microwave generator in order to: a) saturate the MESFET (NEC 71083), b) provide enough power for the frequency doubler and frequency tripler, and c) allow the simulation of any passive load at f_o at the output of the test transistor. A frequency doubler and a frequency tripler should provide sufficient harmonic power to permit the simulation of any passive load at each harmonic which might be seen by the MESFET. The bandwidth of the branch phase/amplitude controllers is lower than the required six-port reflectometer bandwidth. The gate of the MESFET is biased by means of a T junction placed before the test fixture. However, the T junction used to bias the drain is placed at the output of port 3 of SP2 because inside SP2, a DC connection is available between Port 3 and its measuring port. A block diagram of the measurement system for multi-harmonic load pull is shown in Figure 1. The extension of this measurement system to investigate higher harmonics is straightforward by adding more harmonic branches and by using appropriate dividing/filtering circuits before power detection.

EXPERIMENTAL RESULTS

Experimental measurements were performed on a NEC 71083 MESFET operated in Class AB with a driving input power level of 4 dBm at 2.4 GHz and 3.6 GHz. Polarization voltages and current are as follows: $V_{ds} = 3$ volts, $I_{ds} = 10$ mA and $V_{gs} = -0.24$ volts. The measurements include:

- 1) $P_{in}(f_o)$: power input to the test transistor obtained by SP1.
- 2) $P_L(f_o)$: the power delivered to load impedance $Z_L(f_o)$, obtained by SP2.
- 3) $P_L(n f_o)$: the harmonic power delivered to the harmonic load impedance $Z_L(n f_o)$, obtained by SP2.

- 4) $\Gamma_{in}(f_o)$: the large signal input reflection coefficient, obtained by SP1.
- 5) $\Gamma_L(f_o)$: the reflection coefficient associated with the load seen by the transistor $Z_L(f_o)$, obtained by SP2.
- 6) $\Gamma_L(n f_o)$: the reflection coefficient associated with the harmonic load seen by the transistor $Z_L(n f_o)$, obtained by SP2.
- 7) I_{ds} : the DC drain current measured by a milliammeter.
- 8) V_{gs} : the DC gate voltage measured by a voltmeter.
- 9) V_{ds} : the DC drain voltage measured by a voltmeter.

In this paper, only the second and third harmonic loadings are investigated ($n = 2$ and 3). The input matching network is a mechanical tuner with a given stub position to match the source impedance to the transistor input impedance for the input driving level of 4 dBm (see Figure 1). The transistor NEC 71083 is placed in an appropriate fixture and the de-embedding is done using the TRL method [8].

Figure 2 shows conventional constant power contours $P_L(f_o)$ in $\Gamma_L(f_o)$ plane where the value of $\Gamma_L(2f_o)$ and $\Gamma_L(3f_o)$ were set at $.22 \times 53^\circ$ and $.52 \times 113^\circ$ respectively. The power-added efficiency (n_a) contours corresponding to Figure 1 are obtained using the following equation:

$$n_a = 100\% \frac{P_L - P_{in}}{P_{dc}} \quad (1)$$

where,

- P_L : is the microwave power delivered to load (mw)
 P_{in} : is the microwave power input to the transistor (mw)
 P_{dc} : is the DC power delivered to the transistor (mw)

P_{dc} is calculated as follows:

$$P_{dc} = I_{ds} V_{ds} \quad (2)$$

Figure 4 shows constant power contours $P(2f_o)$ in the $\Gamma_L(f_o)$ plane. It is seen that the optimum load for frequency doubling lies in the region $\Gamma_L = .9 \times 70^\circ$ (area of maximum power level at $2f_o$), and the optimum load as an amplifier lies in the region $\Gamma_L = .5 \times 20^\circ$ (area of minimum power at $2f_o$). It is also seen that the load for amplifier maximum efficiency given by Figure 3 corresponds to a minimum power at the second harmonic (Fig. 4) for the given bias test conditions. Figure 5 shows constant power contours $P_L(2f_o)$ in the $\Gamma_L(2f_o)$ plane for fixed value of $\Gamma_L(f_o)$ and $\Gamma_L(3f_o)$ respectively set at $.64 \times -29^\circ$ and $.52 \times 113^\circ$. It is found that the

maximum power level at the second harmonic lies in the region $.5 \times 160^\circ$. Figure 6 shows constant power contours $P_L(3f_o)$ in the $\Gamma_L(3f_o)$ plane for fixeds value of $\Gamma_L(f_o)$ and $\Gamma_L(2f_o)$ respectively set at $.84 \times 29^\circ$ and $.21 \times 120^\circ$. It is to be noted that two operating frequency points were chosen for f_o , namely: 2.4 GHz and 3.6 GHz. The input power, P_{in} is kept constant, ($P_{in} = 4$ dBm) during all the above measurements.

The experimental points in Figures 5 and 6 lie on quasi-circles indicating that harmonic loading has little effect on harmonic generation processes. However, harmonic impedances are important in determining the harmonic power coupled to the output circuit. Furthermore, harmonic impedances are also important in optimizing the efficiency of MESFET working on an amplifier for a given and fixed output power. It is expected that MESFET multi-harmonic load-pull characterization permits an accurate determination of the most important non linear elements in MESFET models such as C_{gs} , C_{ds} and I_d [9] by using appropriate non linear simulator (e.g. harmonic balance) and optimizing routines.

CONCLUSION

A new multi-harmonic load-pull method is presented in this paper. It is seen that this method can be very useful for designing non linear circuits such as high power amplifiers or frequency doublers. It provides the quantitative data on the fundamental and harmonic load impedances required to obtain a given performance from a MESFET. This information can then be used to design the most suitable circuit for high power amplifiers or for MESFET frequency doublers. Furthermore, it is expected that such multi-harmonic characterization could be very useful for MESFET non linear modeling.

ACKNOWLEDGEMENT

The author would like to thank Mr. Gilles Brassard of SPAR Aerospace Ltd. for his participation in helpful discussions and for his valuable suggestions.

REFERENCES

- [1] J. M. CUSACK et al, "Automatic Load Contour Mapping for Microwave Power Transistors", IEEE Trans. on Microwave Theory and Techniques, Vol. MTT-22, pp. 1146-1152, December 1974.
- [2] Y. TAKAYAMA, "A New Load-Pull Characterization Method for Microwave Power Transistors", IEEE MTT-S Int. Microwave Symposium Digest, pp. 218-220, June 1976.
- [3] R. STANCLIFF and D. POULIN, "Harmonic Load-Pull", IEEE MTT-S, Int. Microwave Symposium Digest, pp. 185-187, 1979.
- [4] V. LOTT, "A Method for Measuring Magnitude and Phase of Harmonics Generated in Non Linear Microwave Two-Ports", IEEE MTT-S, Int. Microwave Symposium Digest, pp. 225-228, 1988.
- [5] G. F. ENGEN, "The Six-Port Reflectometer an Alternative Network Analyzer", IEEE Trans. on Microwave Theory and Techniques, Vol. MTT-25, pp. 1075-1083, 1977.
- [6] T. E. HODGETTS and G. J. GRIFFIN, "A Unified Treatment of the Six-Port Reflectometer Calibration Using the Minimum of Standards", Royal Signals and Radar Establishment, Report No. 83003, 1983.
- [7] F. M. GHANNOUCHI, R. G. BOSISIO, Y. DEMERS, "Load-Pull Characterization Method Using Six-Port Techniques", IEEE I&M Technology Conference, Washington, D.C., Conference Report pp 536-539, April 1989.
- [8] G. F. ENGEN and C. A. HOER, "Thru-Reflect Line: An Improved Technique for Calibrating the Dual Six-Port Automatic Network Analyzer", IEEE Trans. on MTT, Vol. 27, No. 12, pp. 987-993, December 1979.
- [9] L. O. CHUA and Y. W. SING, "Non-Linear Lumped Circuit Model of GaAs MESFET", IEEE Trans. Electron Devices, Vol. ED-30, p. 825, 1983.

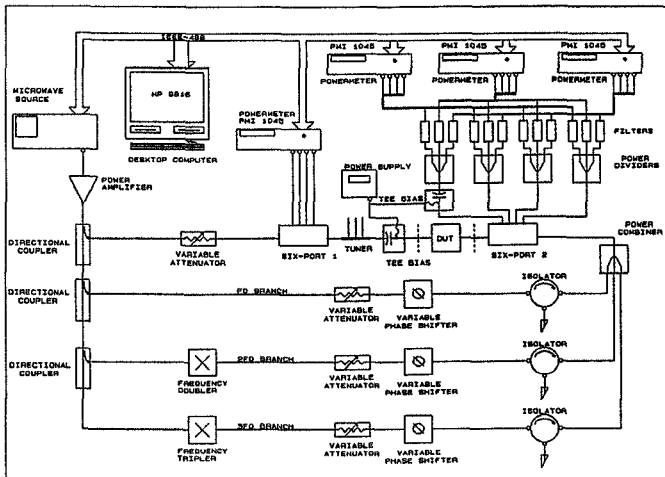


Figure 1

Experimental block diagram of multi-harmonic load-pull system.

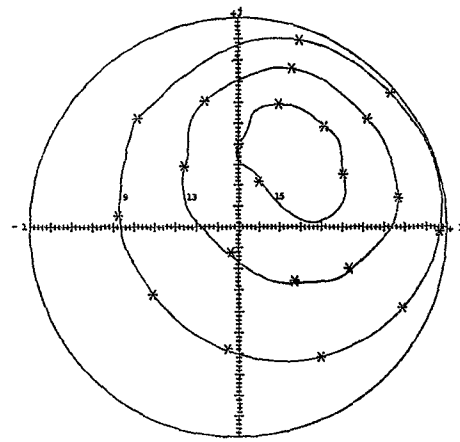


Figure 2

Constant power contours $P_L(f_0)$ expressed in dBm in the complex $\Gamma_L(f_0)$ plane ($f_0 = 3.6$ GHz)

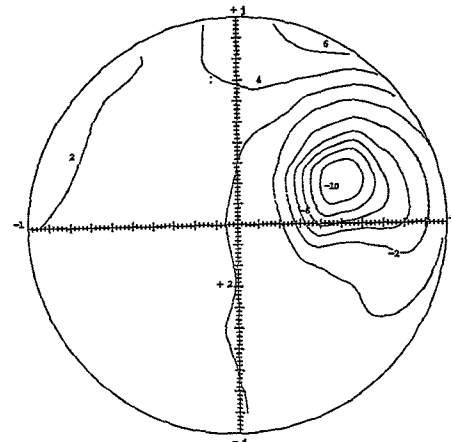


Figure 4

Constant power contours $P(2f_0)$ expressed in dBm in the complex $\Gamma_L(f_0)$ plane ($f_0 = 3.6$ GHz)

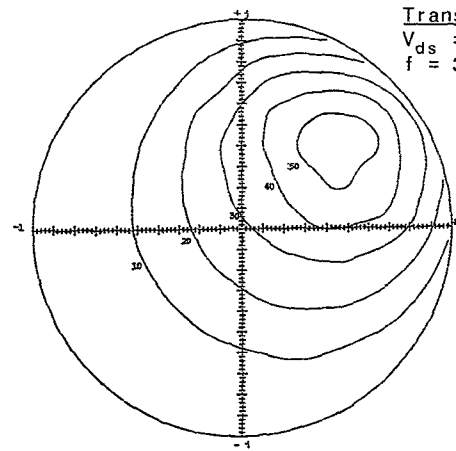


Figure 3

Power-added efficiency contours expressed as a percentage in the complex $\Gamma_L(f_0)$ plane ($f_0 = 3.6$ GHz)

Transistor NEC 71083
 $V_{ds} = 3$ V, $I_{ds} = 10$ mA, $V_{gs} = -0.24$ V,
 $f = 3.6$ GHz, $P_{in} = 4$ dBm

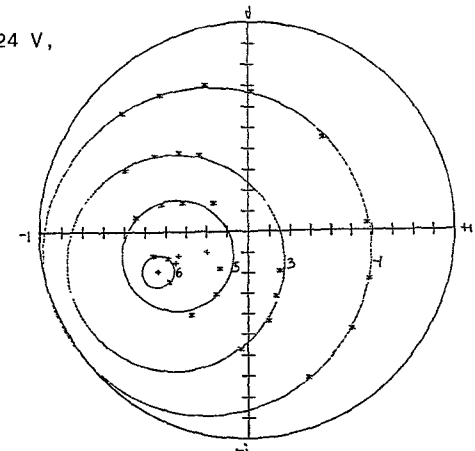


Figure 5

Constant power contours $P_L(2f_0)$ expressed in dBm in the complex $\Gamma_L(2f_0)$ plane ($f_0 = 3.6$ GHz)

Figure 6

Constant power contours $P_L(3f_0)$ expressed in dBm in the complex $\Gamma_L(3f_0)$ plane ($f_0 = 2.4$ GHz).

Transistor NEC 71083
 $V_{ds} = 3$ V, $I_{ds} = 10$ mA, $V_{gs} = -0.24$ V,
 $f = 2.4$ GHz, $P_{in} = 4$ dBm

